J. Physiol. (1974), **238**, *pp.* 55–77
With 1 *plate and* 8 *text-figures*
Printed in Great Britain

ANALYSIS OF NON-LINEARITY OBSERVED IN THE CURRENT–VOLTAGE RELATION OF THE TUNICATE EMBRYO

BY SHUN-ICHI MIYAZAKI,* KUNITARO TAKAHASHI, KAZUKO TSUDA† AND MITSUNOBU YOSHII

From the Department of Neurophysiology, Institute of Brain Research, School of Medicine, University of Tokyo, Tokyo, Japan

(*Received 6 August 1973*)

SUMMARY

1. In the gastrula of the tunicate (*Halocynthia aurantium*) the resting potential of the embryonic membrane was about −70 mV in both std ASW and Na-free ASW.

2. The potential responses to depolarizing current in the early gastrula embryo showed distinct potential jumps from about −50 to about +40 mV during the application of current and from about 0 to resting level after its cessation thus forming a plateau at about 0 mV. Those jumps were not altered significantly by the removal of both Na and Ca ions from ASW except for the duration of the plateau after the cessation of current.

3. Blastomeres in an embryo were tightly coupled with each other electrotonically at the blastula and gastrula stages. The fact that the coupling ratio was nearly 1·0 made it reasonable to treat an embryo as one cell as far as electrical properties are concerned.

4. The I–V relation of the embryonic membrane consisted of an inward rectifying region, outward rectifying region and transitional zone between the two, resulting in a S-shaped curve as in the egg cell membrane. But in the gastrula embryo, the transitional zone actually included the discontinuous part of the I–V curve (from about −50 to about +40 mV) due to the potential jump.

5. The ionic current (I_i) during the potential jump in Na-free ASW was estimated from the slope of the potential response based on the assumption of constant capacitance during the membrane potential changes. The

Present address:
* Department of Physiology and Neurosciences, School of Medicine, Stanford University, Stanford, California, U.S.A.
† Section of Neurophysiology, Tokyo Metropolitan Institute for Neurosciences Tokyo, Japan.

calculated I_i–V curve complemented the interrupted I–V curve smoothly and showed the existence of a negative resistance region from about -50 to about 0 mV in the steady-state I–V relation.

6. The steady-state I–V relation was altered significantly by changing the K concentration in ASW, and the existence of the negative resistance can be reasonably explained by the marked inward-going rectification or anomalous rectification of K conductance.

7. The replacement of K with Rb in ASW produced the marked suppression of the inward-going rectification of the embryonic membrane.

INTRODUCTION

As described in the preceding paper (Miyazaki, Takahashi & Tsuda, 1974), a marked non-linearity in current–voltage relation exists in the egg cell membrane of the tunicate. The non-linearity includes both inward- and outward-going rectifications in different ranges of the membrane potential.

The inward-going rectification has been known as anomalous rectification in vertebrate striated muscle (Katz, 1949; Hodgkin & Horowicz, 1959; Nakajima, Iwasaki & Obata, 1962; Adrian & Freygang, 1962*a*; Adrian, Chandler & Hodgkin, 1970) and in cardiac muscle (Hall, Hutter & Noble, 1963; Hutter & Noble, 1960; Noble, 1965; Noble & Tsien, 1968), or as K inactivation in the electroplaque of the eel (Grundfest, 1960, 1961, 1966; Nakamura, Nakajima & Grundfest, 1965). The functional significance of the inward-going rectification is not known. However, in order to elucidate the embryonic origin of the rectifying properties of the excitable membrane, it is interesting to examine the nature of the inward-going rectification in the embryonic membrane.

In the present paper, special attention has been given to the electrical properties of the embryonic membrane at stage of the gastrula, when the membrane shows the most remarkable inward-going rectification than any other developmental stage of this embryo (Takahashi, Miyazaki & Kidokoro, 1971; Miyazaki, Takahashi & Tsuda, 1972).

METHODS

Collection of the materials were described in the previous paper (Miyazaki *et al.* 1974). The tunicates in the present experiments were exclusively *Halocynthia aurantium* Pallas. In order to obtain the gastrula embryo, the fertilized egg was incubated for 12–24 hr in 6–7° C sea water under continuous aeration. The identification of the embryonic stages and the penetrated cells in an embryo was done in accordance with description in Conklin's map (Conklin, 1905). The methods of recording and exchanging various salines (ASWs) were the same as described in the previous paper (Miyazaki *et al.* 1974). The ASWs used in the present experiments were listed in Table 1.

TABLE 1. Ionic composition of the artificial sea water

ASW	Na	K	Rb	Ca	Mg	Cl	Tris
Standard	452	9·8	—	10·6	48	579	*—
Na-free	—	9·8	—	10·6	48	461	570
106 Ca, Na-free	—	9·8	—	106	48	546	390
106 Ca	309	9·8	—	106	48	627	*—
1·06 Ca, Na-free	—	9·8	—	1·06	48	453	588
Ca- and Na-free	—	9·8	—	—	48	452	590
39 K, Na-free	—	39·2	—	10·6	48	469	533
2·5 K, Na-free	—	2·45	—	10·6	48	459	579
2·5 K, 106 Ca, Na-free	—	2·45	—	106	48	544	399
10 K, Na-free	—	10	—	10	50	498	552
40 K, Na-free	—	40	—	10	50	504	516
100 K, Na-free	—	100	—	10	50	516	444
10 Rb, Na-free	—	—	10	10	50	498	552
40 Rb, Na-free	—	—	40	10	50	504	516
100 Rb, Na-free	—	—	100	10	50	516	444

m-mole/l., pH 7·8–8·0.
* 10 mM Tris HCl, pH 8·0, was added.

RESULTS

Pl. 1 illustrates an early gastrula and an elongated gastrula of *Halocynthia aurantium* Pallas. The present experiments concern the embryos at these stages.

Electrical responses in standard ASW. At the stage of the gastrula the embryonic membrane showed the resting potential of about −70 mV. The responses to depolarizing and hyperpolarizing currents are illustrated in the records of Text-fig. 1*a*, std ASW. The steady-state *I–V* curve of the same embryo is also illustrated in Text-fig. 2*a*, std ASW. The response to the hyperpolarizing current was passive electrotonic and the time course of the potential was roughly exponential (record 1, std ASW). However, a close inspection revealed a slight undershoot of the potential response at the beginning of current application but no overshoot at the cessation of currents. Although the actual time course was not exact exponential, the time required to attain (1–1/e) of the peak response was 0·055 sec for the case of Text-fig. 1*a*, std ASW, record 1. The *I–V* curve was almost linear in the range more negative than the resting potential, although there was a slight upward curvature. The slope resistance at −80 mV was 2·9 MΩ in Text-fig. 2*a*, std ASW (for collected values, see Table 2).

As shown in Text-fig. 1*a*, std ASW, record 2, the response to depolarizing current of intensity less than $0{\cdot}65 \times 10^{-9}$ A was also passive electrotonic potentials but their time course was not exponential. The initial rapid rise of potential within a second was followed by a creeping rise reaching a

TABLE 2. Electrical parameters of gastrula embryos (*Halocynthia aurantium*) (means and S.D.)

Stage	Resting potential (mV)		Slope R (MΩ)[a]		Total capacity (10^{-9} F)		Critical level (mV)[b]	
	std ASW	Na-free	std ASW	Na-free	std ASW	Na-free	std ASW	Na-free
Early stage gastrula	−69 (2) ±3·0	−70·0 (1)	3·92 (2) ±0·81	3·00 (1)	11·7 (2) ±2·3	14·5 (1)	−52·5 (2) ±2·5	−54·0 (1)
Middle stage gastrula	−68·5 (13) ±2·8	−68·6 (9) ±7·0	3·04 (13) ±0·84	2·83 (9) ±0·71	13·0 (11) ±1·8	14·1 (9) ±1·1	−53·5 (12) ±2·7	−52·9 (9) ±6·6
Elongated gastrula	−67·5 (6) ±2·5	−79·2 (3) ±7·4	3·05 (6) ±0·89	3·00 (2) ±0	17·0 (4) ±1·5	19·3 (3) ±1·4	−53·7 (8) ±2·8	−60·0 (3) ±2·0

Parentheses, the number examined.
Temp. 1–4° C.
a, measured at the resting or hyperpolarized level; b, critical level for the potential jump.

steady level after several seconds. This deviation from an exponential time course is explained by the change of slope resistance with membrane potential. The slope resistance at −65 mV was about 20 MΩ, while it was 4 MΩ at −73 mV, the resting potential level. There was inward-going rectification at the potentials more negative than about −60 mV. When

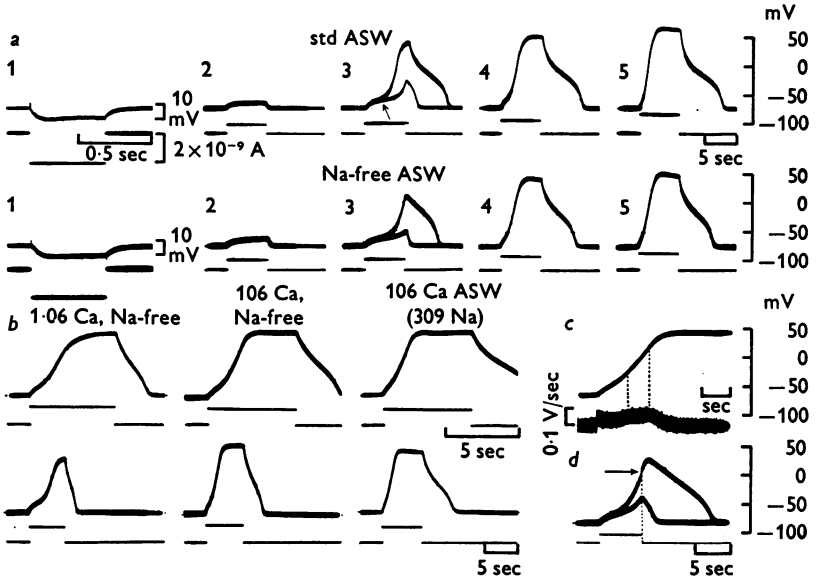

Text-fig. 1*a* illustrates the potential responses to constant current stimulation at gastrula stage in std ASW and Na-free ASW. Temp. 2·5° C. They were obtained from a gastrula embryo with moderately opened blastopore. The resting potentials of the embryo were −73 mV, in std ASW and −76 mV in Na-free ASW. Upper and lower traces in each record illustrate potential and current records respectively in this Figure and in all following Figures. The scales for voltage except those in records 1 std and Na-free ASW indicate also the level of zero membrane potential in this and succeeding Figures. The current scale at record 1 std ASW applies for all records in Text-fig. 1*a*, *b*, *c* and *d*. The arrow in record 3 std ASW indicates the point of mathematical inflexion of the potential response. *b* illustrates effects of enhancement of Ca concentration from 1·06 to 106 mM in Na-free ASW and of restoration of the Na in the presence of 106 mM-Ca on rising and falling phases of the depolarizing response. A late stage gastrula of an elongated gastrula. Temp. 2–3° C. The records in the same column were taken in the same external medium and the records in the same line were obtained by applying the similar amount of current. *c* illustrates the rate of rise during the rising phase of depolarization in 106 Ca ASW with 309 mM-Na. The same embryo as in part *b*. *d* illustrates the regenerative response of a late stage gastrula or an elongated gastrula occurring in the selected ionic environment of 2·45 mM-K, 106 mM-Ca and Na-free ASW. The arrow indicates the critical level for the regenerative response. Temp. 6·5° C.

the depolarizing current was slightly over the critical value of $0{\cdot}65 \times 10^{-9}$ A, the membrane depolarization showed an inflexion point (see p. 68) at -58 mV as indicated by an arrow in record 3. No steady value of the potential was obtained above -58 mV and the depolarization increased continuously up to the level of $+40$ mV. Accordingly, the I–V curve showed distinct transition from -58 to $+40$ mV at critical current of $0{\cdot}65 \times 10^{-9}$ A (interrupted line in Text-fig. 2*a*, std ASW). The I–V curve

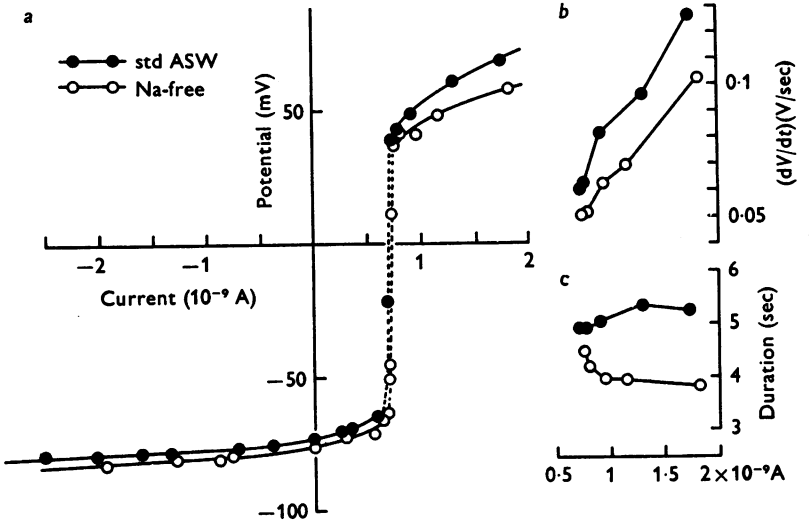

Text-fig. 2*a* illustrates the I–V relations of the embryonic membrane of the same gastrula embryo as illustrated in Text-fig. 1*a* in both std and Na-free ASW. Temp. 2·5° C. Ordinate is the membrane potential and the abscissa is the applied current in this and subsequent Figures. The interrupted line indicates the portion of the I–V curve where the steady-state membrane potential was not obtained within 6 sec, in this and subsequent figures. *b*, the maximum rate of rise during the potential jump is plotted against the applied current in std ASW (●) and in Na-free ASW (○). *c*, the duration of the falling phase of the depolarizing response after the current cessation was measured at -40 mV level and is plotted against the applied current.

for currents above $0{\cdot}65 \times 10^{-9}$ A or potentials above $+40$ mV showed a slope resistance of about 20 MΩ. Closer inspection revealed outward-going rectification in this region of the I–V curve. The potential decay after the cessation of depolarizing current was also far from exponential, and it formed a distinct hump below 0 mV level.

The S-shaped configuration of the I–V curves, thus, was similar to that at egg cell stage described in the previous paper (Miyazaki *et al.* 1974). The quantitative differences between these two curves were as follows:

(1) The potential jump appeared in the negative direction for -20 m to -60 mV with the hyperpolarizing current in the case of two cell embryo shown in Text-fig. 3*a*, std ASW of the previous paper (Miyazaki *et al.* 1974), while it was elicited from -58 to $+40$ mV with depolarizing current at the stage of the gastrula (Text-fig. 2*a*). (2) The critical currents were $0{\cdot}4 \times 10^{-10}$ A in the two cell embryo in Text-fig. 3*a*, std ASW of the previous paper and $6{\cdot}5 \times 10^{-10}$ A in the gastrula embryo in Text-fig. 2*a*, std ASW. (3) The limiting slope resistance in the inward rectifying region of the *I–V* curves was less for the gastrula than for the two cell stage embryo, the values being 2·9 MΩ for the gastrula and 25 MΩ for the two cell embryo of Text-fig. 3*a* in the previous paper.

Electrotonic coupling among blastomeres in an embryo. Electrical coupling between the blastomeres has been demonstrated in many different embryos including those of amphibia (Ito & Hori, 1966; Ito & Loewenstein, 1969; Slack & Palmer, 1969; Palmer & Slack, 1970; Warner, 1970; Bennett & Trinkaus, 1970), the chicks (Sheridan, 1966, 1968, 1971), the echinoderms (Tupper, Saunders & Edwards, 1970), and squid (Potter, Furshpan & Lennox, 1966). All except early stage embryos of the echinoderm (Ashman, Kanno & Loewenstein, 1964; Tupper *et al.* 1970) have been reported to show extremely tight coupling with a coupling ratio of almost 1·0. In this tunicate embryo, the responses to the current pulses were the same in any blastomeres of an embryo at the initial stage of blastula and at the stage of gastrula. It is expected that the whole embryo behaves electrically as one cell with tight electrotonic coupling.

In the experiment shown in Text-fig. 3, the one electrode was placed in the blastomere of the muscle region (V_1) and the second electrode was introduced into the blastomere located in the ectodermal region (V_2). Clearly the responses of V_1 were the same as those of V_2 to the current injection through either the V_1 or V_2 electrode (Text-fig. 3*a*).

Plotting V_2 at the end of current pulses against V_1 showed that the coupling ratio (V_2/V_1) between two blastomeres was 1·0 in any ranges of the membrane potential. The same results were obtained at the initial stage of blastula as well.

Ca and Na components in the depolarizing responses. On the removal of Na ions from ASW, the resting potentials remained unchanged or shifted slightly (by less than 10 mV) in the negative direction. The potential jump under the constant current application and the *I–V* curve were almost the same as those in std ASW (Text-figs. 1*a* and 2*a*). Only the critical current necessary to initiate the potential jump was slightly (0–30 %) larger than that in std ASW. In the gastrula embryo, the inflexions due to both Na and Ca regenerative response were usually not clear because of the superposition of the steep potential jump initiating from about

– 55 mV. However, the plotting of the maximum rate of rise during the jump and the duration of the falling phase after the current cessation against current intensity in both std ASW and Na-free ASW indicates that the distinct effects of the Na removal were in the decrease of both amounts (Text-fig. 2*b*, *c*). This fact suggests that Na inward current was included in the embryonic membrane at the gastrula stage as well.

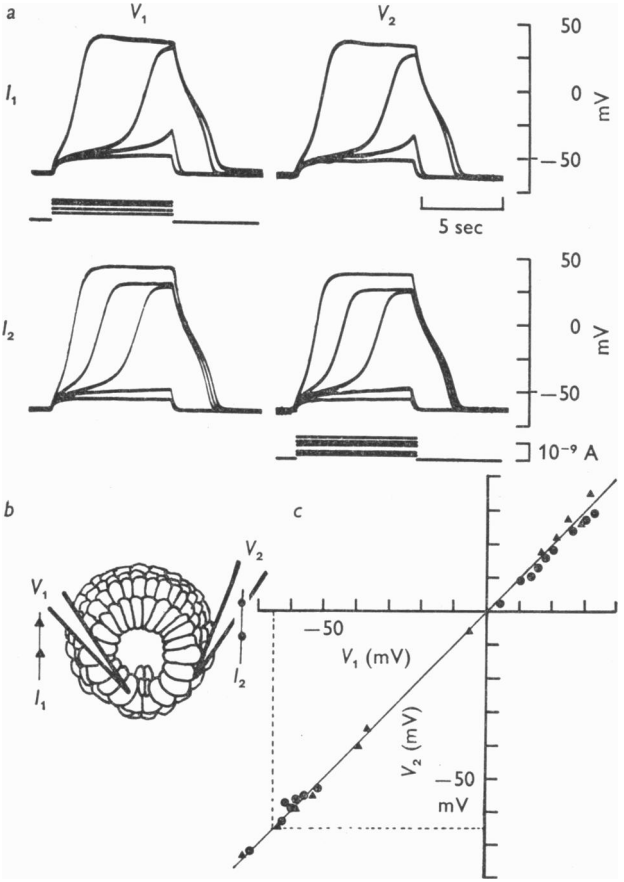

Text-fig. 3. A demonstration of the electrotonic coupling among blastomeres with two micro-electrodes (V_1 and V_2) in a gastrula embryo with a widely opened blastopore. *a* illustrates the potential responses of V_1 and V_2 to depolarizing currents through V_1 electrode (I_1) and through V_2 electrode (I_2). *b* illustrates the location of the electrodes. V_1 electrode was in the blastomere of the presumptive muscle area and V_2 electrode was in the blastomere of the presumptive ectodermal area. *c* illustrates the relation between V_1 and V_2 potentials either with current through V_1 electrode (filled circle) or with current through V_2 electrode (filled triangles). Note the straight line through the origin with 45° slope. Interrupted lines indicate the resting level.

In order to demonstrate Ca contribution to the response clearly, the Ca concentration was preliminarily reduced to one tenth of the standard, i.e. 1·06 mM in Na-free condition and then Ca content was increased from 1·06 to 106 mM, and finally Na ions were replaced keeping the Ca concentration at the same level (Text-fig. 1*b*). The responses to depolarizing currents of the similar intensities were compared successively in three solutions, starting from the same resting potential in each case. Although the final potential level was similar in the three solutions, the sharp shoulder on the rising phase appeared only in the high Ca condition. The rate of rise during the depolarization in 106 Ca ASW with 309 mM-Na showed two maxima (interrupted lines) at the level of -30 and $+15$ mV. The latter probably corresponds to the Ca current, while the former may include the Na current (Text-fig. 1*c*). As described above, the presence of sodium caused a prolongation of the falling phase. It should be noted that high Ca also lengthened the falling phase. However, even in 1·06 mM-Ca and Na-free condition a distinct hump on the falling phase was still observed. The durations of the falling phase measured at -40 mV were 1·8, 2·3 and 3·3 sec in 1·06 Ca, 106 Ca, and 106 Ca in the presence of Na.

Further evidence for Ca component in the depolarizing response at the gastrula stage was the elicitation of a regenerative response under the selected ionic environment of 10 times Ca and one fourth K concentration (106 Ca, 2·5 K, Na-free ASW) as shown in Text-fig. 1*d*. The critical level for Ca action potential was $+5$ mV (horizontal arrow), the value being similar to that in the egg cell membrane described in the previous paper (Miyazaki *et al.* 1974).

In summary, both Na and Ca components were suggested in the depolarizing response of the gastrula but neither characteristic potential jump nor non-linear $I-V$ relation was influenced by the deficiency of Na or Ca ions.

Although decoupling of the electrotonic connexion between cells has been reported to result from a deficiency of the divalent ions Ca and Mg (Loewenstein, 1968; Loewenstein, Nakas & Socolar, 1967; Rose & Loewenstein, 1971), no sign of decoupling was found by observing electrotonic spread of potential with 1 mM-Ca and 48 mM-Mg in ASW.

Analysis of the non-linearity in the current–voltage relations. Since the potential jump was independent of both Na and Ca, it is likely that the negative resistance exists in some portion of the $I-V$ relation and produces the jump on the application of the constant current. Therefore, it is important to have the quantitative estimate of membrane currents in the non-linear portion of the $I-V$ curve, especially in the portion hidden by the potential jump, under the condition of the external Na absence.

The generally accepted equivalent circuit for biological membrane has included capacitative and resistive admittances in parallel, so that the first step of the analysis should be in the separation of the membrane current into the resistive (or ionic) and capacitative components during and after application of the extrinsic current. The procedure for the separation can be represented in the following equations:

$$I = (I_1)_R + C(dV/dt)_R, \tag{1}$$

$$O = (I_1)_F + C(dV/dt)_F, \tag{2}$$

where I is the extrinsic current applied through the membrane. V represents membrane potential and C is total membrane capacity. I_1 is the ionic current, $C(dV/dt)$ is the capacitative current and the suffixes R and F represent the quantities obtained during the rising and falling phase of the potential change. Because of the non-linearity in the I–V curve, it is not so simple to estimate the capacity. Therefore, making the assumption that the ionic current is independent of time and dependent only upon the membrane potential in a certain range of the time and potential, that is; $I_1 = f(V)$ and $I_1 \neq f(V, t)$, the ionic current should be equal during either the rising phase or the falling phase, if the measurements are done at the same membrane potential level (V_0), i.e. $(I_1)_{R, V=V_0} = (I_1)_{F, V=V_0}$. Introducing V_0 into V in eqns. (1) and (2) and subtracting the eqn. (2) from eqn. (1), the following equation will be given:

$$I = C\{(dV/dt)_{R, V=V_0} - (dV/dt)_{F, V=V_0}\}. \tag{3}$$

Since $(dV/dt)_F$ is always negative, the sum of slopes from the rising and falling phases at the same potential level is linearly proportional to the applied current, irrespective of the value of V_0, and the proportionality coefficient between the current and slopes is the capacitative value. Finally, assuming the obtained C value varied beyond the range of the potential which substantiates eqn. (3), the ionic currents at the falling or rising phase can be written as follows:

$$(I_1)_R = (I - C(dV/dt)_R)_{V=V_0}, \tag{4}$$

$$(I_1)_F = (-C(dV/dt)_F)_{V=V_0}. \tag{5}$$

Then the required relation between the I_1 and V in the transitional portion of the curve can be calculated.

Estimation of the ionic current in Na-free ASW. Text-fig. 4*a* illustrates responses of a gastrula embryo to currents of different intensities, used for the calculation. The *a*4 record schematically illustrates how the slope of the potential change was measured. Since the time course of the potential change was extremely slow, the tangent of the response curve at the

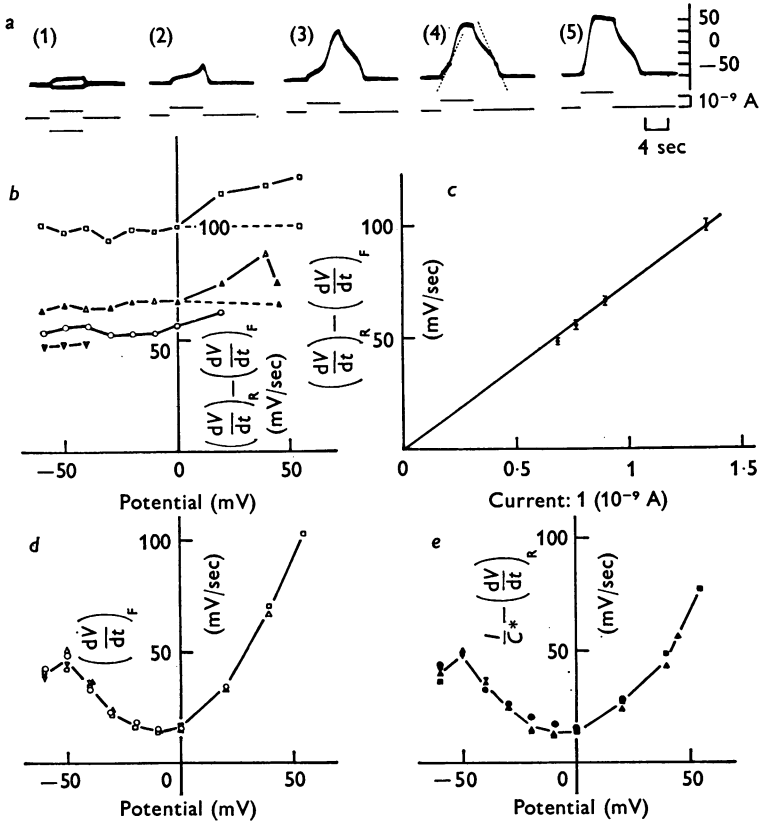

Text-fig. 4. The calculation of ionic current during the potential jump in Na-free ASW. A middle stage gastrula with moderately opened blastopore. Temp. 5·5° C. *a* illustrates the records of analysed potential responses. In *b* the sum of the slopes at rising and falling phases of a potential response is plotted against the membrane potential at which the slopes were measured. Each symbol corresponds to each response evoked by a current of different intensity as indicated by the number at the left side. *c* illustrates the method of estimation of effective capacity of this embryo. The average sum of the slopes in each response is plotted against the intensity of the applied current. The sum obtained above 0 mV level was excluded from the calculation (for explanation see text). The vertical bar indicates S.D. The slope of the straight line through the origin is $1/13{\cdot}9 \times 10^9\ \mathrm{F}^{-1}$. *d* and *e* illustrate calculated ionic currents at rising (filled symbols) and falling (open symbols) phases. The different shaped symbols correspond to the values estimated from responses with different current intensities. The shapes of the symbols are common in parts *b*, *d* and *e*.

desired potential level was drawn directly on the potential trace in the print instead of using the differentiater. The actual measurements of the slopes were done at every 10 mV step of the membrane potential.

In Text-fig. 4*b*, the sum of the slopes at rising and falling phases are plotted against membrane potential. Four curves correspond to four responses to four different current intensities. The sum is found to be constant in the potential range below 0 mV although there is a slight variation probably due to error in measurement. Above 0 mV the sum tends to increase with positive increment because of the time dependent Ca permeability and/or the time-dependent outward-going rectification and partly because of the possible variation of the capacity as a function of the membrane potential.

Besides the usual measurements of slopes at the rising and falling phase, the slopes of the potential response can be estimated infinitesimally before and after current cessation. Using these two slopes, eqn. (3) should be fulfilled regardless of the existence of time dependent permeability or I_1. The sum of these slopes was also plotted against the membrane potential at the end of the current pulse in the case of records 4 and 5. The values of the sum were exactly the same as those obtained below 0 mV as indicated by the interrupted line. This result implies that the variation of the capacity is negligible within the accuracy of the measurement.

In Text-fig. 4*c*, the average and the standard deviation of the sum in each response are plotted against the intensity of the current applied. The data obtained above 0 mV level were excluded from the calculation. As expected, the points formed a straight line passing through the origin. The proportionality coefficient was $1/13{\cdot}9 \times 10^{+9}\ \mathrm{F}^{-1}$, and the constancy of the capacity was proved.

The calculated $(I_1)_F$ and $(I_1)_R$ were plotted against the membrane potential in Text-fig. 4*d*, *e*. The points from the different responses coincided with each other if the measured potential level was the same. This means that I_1 is not dependent on the current applied but upon the potential. As to the time dependence of the I_1, it is convenient to compare the curves of I_1 between rising phase and falling phase since there is time lag between the two phases. As was inferred from the results of Text-fig. 4*b*, the two V–I_1 curves were the same below 0 mV, while above 0 mV the curve from the rising phase showed a slightly smaller outward current at the given membrane potential.

To test the validity of the calculation, both I_1–V curves were superposed upon the usual I–V curve (Text-fig. 5). Although there is a slight difference between the I_1–V and I–V curves above the transitional region, the I_1–V curve connects the two portions of the 'steady' I–V curve, separated by the transitional region, and forms S-shaped curve. This indicates the presence of negative resistance. Further if this construction of the I–V curve is valid, with a conditioning depolarization beyond the potential

jump the steady-state $I-V$ relation should also be obtained in the region of the calculated I_1-V curve above -5 mV, which had a positive resistance. The inset of Text-fig. 5 illustrates the potential response to two steps of depolarizing current, the first one being kept constant as a conditioning depolarization at $+50$ mV (vertical arrow). The open circles plot the final

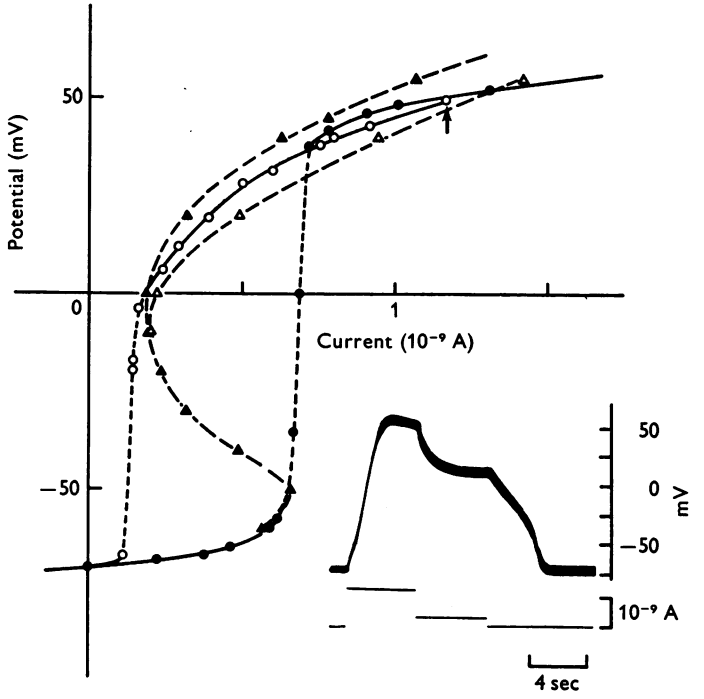

Text-fig. 5. Demonstration of the existense of negative resistance in the steady state $I-V$ relation. The same embryo as illustrated in Text-fig. 4. Na-free ASW. Temp. 5·5° C. Open circles indicate the $I-V$ relation after a conditioning depolarization beyond the jump level superposed on the usual $I-V$ curve (filled circle). The test current was reduced from the conditioning level as shown in the inset. Triangles indicate the same calculated ionic currents at both rising (filled symbol) and falling (open symbol) phase as illustrated in Fig. 5*d* and *e*.

membrane potential as a function of the test current. When the test current intensity became only slightly below the minimum value of calculated ionic current (I_1), the $I-V$ curve abruptly shifted down to the inward rectifying region around the resting membrane potential. In the other words, there was a potential jump to the hyperpolarizing direction in this case. These results validate the completion of the $I-V$ curve, which is defective in the transitional region, by the calculated I_1.

The critical membrane potential for the potential jump has not been defined clearly, because the inflexion induced by the non-linearity in the $I-V$ relation was not so sharp in comparison with that elicited by cationic inward current, such as the 'off response' at early egg cell stages. Considering that the cell membrane has the non-linearity in the instantaneous current–voltage relation $I_i = f(V_m)$, the following equation can describe the electrotonic potential elicited by constant current I,

$$I = I_i + C\frac{dV_m}{dt} = f(V_m) + C\left(\frac{dV_m}{dt}\right). \tag{6}$$

By differentiating the equation (6) on both sides,

$$0 = \frac{d(f(V_m))}{dt} + C\frac{d^2V_m}{dt^2}. \tag{7}$$

If V_c is the maximum steady membrane potential with critical current intensity in the $I-V$ relation, then

$$\left(\frac{dI_i}{dV_m}\right)_{V_m=V_c} = 0. \tag{8}$$

Since

$$\frac{d(f(V_m)}{dt} = \frac{df(V)}{dV_m}\frac{dV_m}{dt}$$

$$\left\{\frac{dV_m}{dt}\frac{d(fV_m))}{dV_m} + C\frac{d^2V_m}{dt^2}\right\}_{V_m=V_c} = \left(\frac{dV_m}{dt}\right)_{V_m=V_c}\left(\frac{dI_i}{dV_m}\right) + C\left(\frac{d^2V_m}{dt^2}\right)_{V_m=V_c} = 0. \tag{9}$$

By considering eqn. (8),

$$\left(\frac{d^2V_m}{dt^2}\right)_{V_m=V_c} = 0.$$

Therefore, if $V_m = V_c$, the response is just on the mathematical inflexion point, Thus, it is convenient to define the critical membrane potential for the potential jump as V_c.

The effects of the external K on the steady-state $I-V$ curve. In the egg cell and the gastrula embryo the inward-going rectification represented by the potential jump occurs independently of both Na and Ca ions. Therefore, it is natural to expect that the property is due to the non-linearity of K conductance in relation to the membrane potential.

Text-fig. 6*c* illustrates the shift of the resting potentials caused by alteration in the external K concentration from 2·45 to 39 mM at the early gastrula stage. The resting potentials were initially −70 mV in std K, Na-free ASW and became −102·5 mV in 2·5 K, Na-free ASW and on exchange of the latter solution with 39 K, Na-free ASW, it became −38 mV (⊙ in Text-fig. 7*a*). The resting potentials of other several gastrula embryos in Na-free ASW are also plotted against the potassium concentration with open circles in Text-fig. 7*a*. A connected pair was obtained in a given embryo. The results show that in Na-free ASW the resting membrane behaves exactly as a potassium electrode. Text-fig. 6*a*

illustrates a series of potential responses to depolarizing and hyperpolarizing currents with increase of K concentration. Beside the evident shift of the resting potential, there were also successive decreases in the critical levels for the potential jump and in the duration of the falling phase (see Table 3).

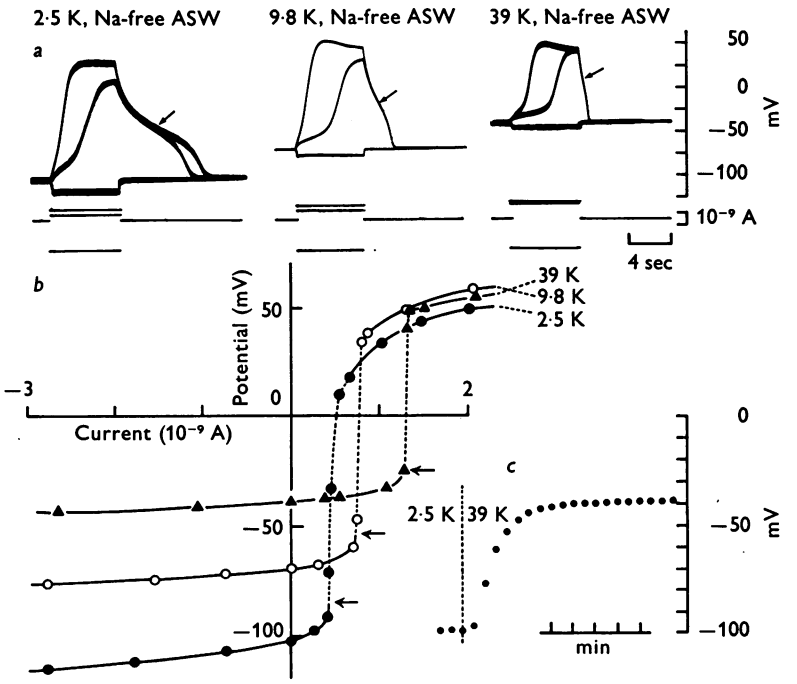

Text-fig. 6*a*. Effects of the enhancement of K concentration on the resting potentials and the potential responses to constant current in Na-free ASW. A gastrula with a widely opened blastopore. Temp. 5° C. The oblique arrows indicate the points of minimal slope during the falling phase. Effects of the enhancement of K concentration on the *I–V* relation in Na-free ASW are shown in *b*. The same embryo as illustrated in *a*. Horizontal arrows indicate the critical membrane potentials for the potential jumps in respective K concentrations. *c* illustrates the shift of the resting potentials during the increment of K concentration from 2·45 to 39 mM in Na-free condition.

Text-fig. 6*b* presents the *I–V* curves of the responses illustrated in Text-fig. 6*a*. The most remarkable modifications of the *I–V* curves in accordance with the successive increase in K concentration are: (1) there is a vertical shift of the inward rectifying region due to decrease in the resting potential, while the upper outward rectifying region beyond the potential jump remains relatively unchanged, or its changes are not consistent with those of K concentration; (2) the transitional region from the

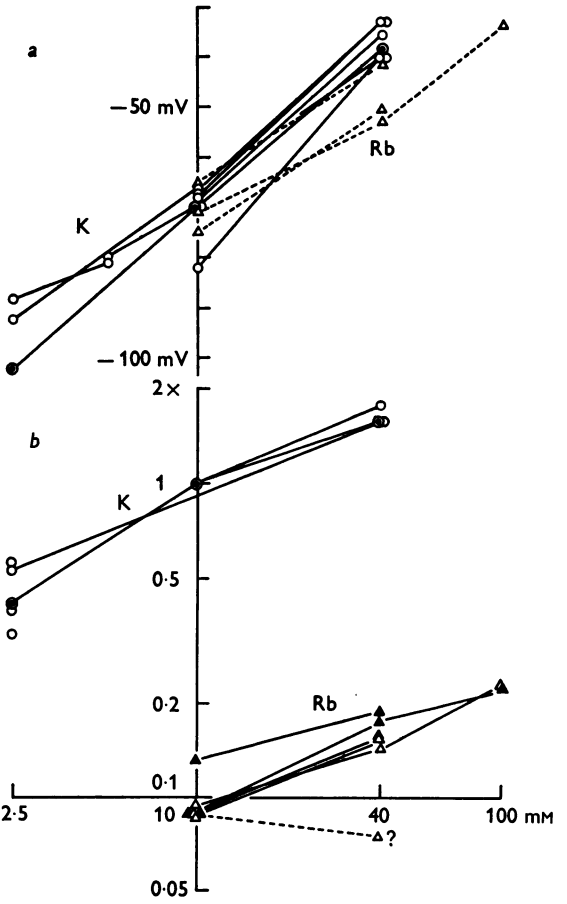

Text-fig. 7*a*. The dependence of resting potentials of gastrula embryos upon the concentration of K (circle) and Rb (triangle) in Na-free ASW. A set of points connected by straight line was obtained with a given embryo. The concentration in logarithmic scale. *b*, the dependence of slope conductances of gastrula embryos upon the concentration of K (circle) and Rb (triangle) in Na-free ASW. The values of slope conductances on the ordinate are represented by the multiples of the slope conductance of the control $I-V$ relation at the zero current condition in 10 K, Na-free ASW of each embryo, except three plots in 2·5 K Na-free ASW which were obtained by the ratio to the average value in 10 K, Na-free. Both abscissa and ordinate are in logarithmic scale. For Rb experiments, open symbols indicate the ratios obtained at the zero current condition and filled symbols those at limiting condition. All data were obtained at temperature 2–6° C. ⊙ indicates the data obtained from the same gastrula embryo illustrated in Text-fig. 6.

inward rectifying portion to the outward rectifying portion shifts horizontally as a result of the increase in the critical current for the potential jump. This can be considered to be a result of the increase in the K conductance due to the increment of the external K concentration. To

TABLE 3. Chord conductance and potassium concentration

K conc. ...	2·45 mM-K	9·8 mM-K	39 mM-K	Conductance ratio
Resting potential (E_K) (mV)	−102·5	−70·0	−38·0	—
Slope resistance (MΩ) at resting level	7·3	3·0	1·9	—
Chord conductance (*a*) (10^{-7} mho)	1·37	3·33	5·26	0·41/1/1·6
Critical level for the jump (E_c) (mV)	−85·0	−54·0	−25·0	—
K electrochemical potential at E_c ($E_c - E_K$) (mV)	17·5	16·0	13·0	—
Critical current (10^{-10} A)	4·1	7·3	12·7	—
Chord conductance (*b*) (10^{-8} mho)	2·34	4·56	9·77	0·51/1/2·1
Minimal slope at the falling phase (mV/sec)	9·75	22·0	56·5	—
Total capacity (10^{-9} F)	13·0	14·5	13·1	Average 13·5
Minimal current (10^{-10} A)	1·32	2·97	7·63	—
K electrochemical potential at the plateau level (E_p) ($E_p - E_K$) (mV)	57·5	50	50	—
Chord conductance (*c*) (10^{-9} mho)	2·30	5·94	15·26	0·39/1/2·6

* All values were obtained in an embryo at the initial stage of the gastrula.

test this point further, the following three types of the chord conductances were calculated as illustrated in Table 3 and compared quantitatively in relation to K concentration. (*a*) The slope conductances at the neighbourhood of the resting potential. They were 1·37, 3·33 and $5{\cdot}26 \times 10^{-7}$ mho in the 2·5, 9·8 and 39 K, Na-free ASW respectively. (*b*) The chord conductances at the level of the critical membrane potential. They were 2·34, 4·56 and $9{\cdot}77 \times 10^{-8}$ mho respectively. (*c*) The chord conductances at the level of the minimal I_1 or minimal slope of the falling phase (arrows in Text-fig. 6*a*). As expected from the reduction in the duration of the falling phase, minimal slopes increased with the increment of the potassium. Thus chord conductances at the minimal current increased successively, being 2·30, 5·94 and $15{\cdot}26 \times 10^{-9}$ mho respectively. The ratios of these three parameters for conductance were calculated for the three different K concentrations, 0·41 : 1·0 : 1·6 for the slope conductance (Text-

fig. 7*b*, ⊙), 0·51:1·0:2·1 for the chord conductance at the critical membrane potential and 0·39:1·0:2·6 for that at minimal I_1. In addition to the fact that the resting membrane in Na-free ASW behaves exactly as a potassium electrode, the rough coincidence of these ratios indicates that the properties of the $I-V$ curve are mainly determined by K conductance and that the K conductance is the electrochemical potential dependent instead of just membrane potential dependent.

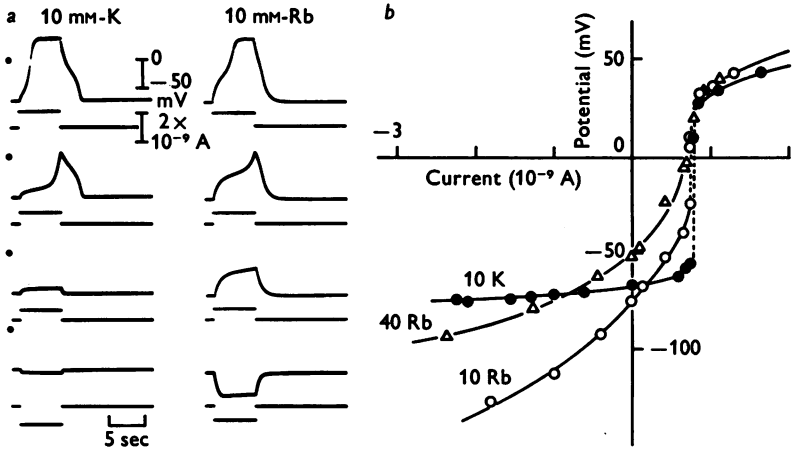

Text-fig. 8*a*. Potential responses to the depolarizing and hyperpolarizing currents in 10 mM-K and 10 mM-Rb in the Na-free condition. An early gastrula embryo, temp. 4–6° C. Each dot in the left side of the record indicates zero potential level. *b* shows $I-V$ relations in 10 mM-K, Na-free ASW (10 K), 10 mM-Rb, Na-free ASW (10 Rb), and 40 mM-Rb, Na-free ASW (40 Rb). The same gastrula embryo as illustrated in part *a*.

In Text-fig. 7*b* the ratios of the slope conductances in the linear range of $I-V$ curve (below −70 mV) to that of std K solution (9·8 mM) are plotted against K concentration with log-log scale. A 4 times increase in external K approximately doubled the slope conductances.

The effects of the replacement of external K with Rb on the I–V relation. It is known that the inward-going rectification of the frog striated muscle is abolished in the Rb-Ringer (Adrian, 1964; Adrian *et al.* 1970). In this tunicate, effects of the replacement of external K with Rb were also examined. On the replacement with Rb ions in Na-free ASW there was the hyperpolarizing shift of the potential by 10–20 mV. In Rb-ASW, the increase in the Rb concentration from 10 to 40 mM produced depolarization of 20 mV and the exchange of 40 mM-Rb ASW with 100 mM-Rb ASW further depolarized the membrane by 18 mV (Text-fig. 7*a*, interrupted line). Therefore, in Rb ASW as in K ASW the resting potentials followed

Nerst equation at least in the concentration above 40 mM although in Rb ASW the relation shifted in hyperpolarizing direction by about 20 mV in average. Assuming that inside K concentration does not change during the exchange of the external solution, the potential difference of about 20 mV at 4–6° C between K ASW and Rb ASW indicates the permeability ratio $P_{Rb}/P_K = 0{\cdot}5$ according to the constant field equation.

Responses to depolarizing and hyperpolarizing currents and *I–V* relations in both K and Rb ASW in a gastrula embryo are illustrated in Text-fig. 8*a*, *b*. The electrotonic potentials with hyperpolarizing currents in Rb ASW increased almost by 10 times of those in K ASW. Thus inward-going rectification was markedly suppressed. With depolarizing currents there is also a potential jump, but the critical membrane potential for the jump was much less negative than in K ASW, being -25 mV in 10 mM-Rb ASW and -55 mV in 10 mM-K ASW. By increasing Rb concentration from 10 to 40 mM, the electrotonic potential to the hyperpolarizing current reduced to an approximately half. Therefore, the slope conductances in Rb ASW were also proportional to the square root of the concentration as in the case of K ASW (Text-fig. 7*b*). The fact that the slope conductances at both zero current and limiting condition in Rb ASW were one tenth of those in K ASW (Text-fig. 7*b*) indicates the conductance ratio $G_{Rb}/G_K = 0{\cdot}1$. The large discrepancy between the permeability ratio and the conductance ratio suggested that the independence principle does not hold for this inward-going rectifying conductance.

DISCUSSION

The non-linearity of the *I–V* curve in the embryonic membrane of the tunicate egg has been described in the preceding paper (Miyazaki *et al.* 1973). Inward-going rectification was dominant in the *I–V* curve at the stage of gastrula. The calculation of the membrane current from the slopes of the potential change showed clearly the negative resistance in the transitional zone between the inward and outward rectifying regions of the *I–V* curve. The contribution of K conductance to this non-linearity has been deduced from the following facts. First, the non-linearity of the *I–V* curve existed equally in Ca-deficient and Na-free ASW as in std ASW. Secondly, three chord conductances at the various points of *I–V* relation were altered in parallel with increase of K content in Na-free ASW.

The *I–V* curves in 2·5 K, 9·8 K, and 39 K solution crossed each other at the gastrula stage (Text-fig. 6*b*). In cardiac Purkinje fibres, marked anomalous rectification of the K conductance has been demonstrated (Weidmann, 1955; Hutter & Noble, 1960; Carmeliet, 1961; Trautwein & Kassebaum, 1961; Hall, Hutter & Noble, 1963; Deck & Trautwein, 1964).

Crossing of the $I-V$ curves in Na-free solutions of different K contents has been observed experimentally, and theoretical treatment based on the assumption that K permeability is dependent upon its electromotive force has predicted each crossing (Hall *et al.* 1963; Noble, 1965). Similarly, it is well known in cardiac Purkinje fibres that the shortening of the plateau of the action potential results from the increase in the external K concentration. A low external K concentration of 2·5 mM sometimes triggers a low resting potential as a consequence of the failure of the evoked action potentials to repolarize (Weidmann, 1956; Noble, 1965). A reduction of the falling phase with increase in the K concentration evidently exists also in this tunicate embryo as illustrated in Text-fig. 6*a*. A similar cross of $I-V$ curves of frog skeletal muscle has been demonstrated in K sulphate solution (Adrian, 1969).

The negative resistance in the K conductance is concluded to evoke the distinct potential jump during constant current application at the gastrula stage. Although no marked negative resistance has been found in either the skeletal or cardiac muscle (Noble, 1965; Adrian, 1964, 1969), the detailed voltage clamp analysis of one component of K conductance has revealed a negative resistance in the instantaneous $I-V$ relation (Adrian & Freygang, 1962*b*; Noble & Tsien, 1968; Adrian, Chandler & Hodgkin, 1970). In amphibian striated muscle, a potential jump is elicited when there is high Cl ions content in the intracellular compartment. It has been suggested that the inward-going rectification of the K conductance will help the jump, but the influx due to other cations or efflux due to an anion, such as chloride, is assumed to be primarily responsible for the jump (Nakajima *et al.* 1962; Adrian & Freygang, 1962*a*). In the electroplaque membrane of the eel and electric fish, the existence of such negative resistance has been demonstrated by voltage clamp (Nakamura *et al.* 1965; Bennett & Grundfest, 1966). With constant current stimulation, the potential jump is also elicited in electroplaque membrane (Nakamura *et al.* 1965; Bennett & Grundfest, 1966). It should be noted that the potential jump caused by negative resistance due to a K conductance decrease will never develop into a regenerative response (Nakamura *et al.* 1965). The K chord conductance should always be positive and the apparent inward-directed current due to negative resistance never becomes a true inward current without coexistence of other ionic currents with different electromotive force than K. Actually in Na-free ASW the potential jump was never maintained after the cessation of the extrinsic current in the tunicate gastrula.

It has been suggested that the anomalous rectification or inward-going rectification in the striated muscle has been assigned to the specific properties of the tubular system membrane (Adrian & Freygang, 1962*a*;

Adrian, 1969). On the other hand, the detubulated muscle has been reported to show the anomalous rectification (Eisenberg & Gage, 1969). In the gastrula embryo or in the egg cell no special internal membrane system which might be comparable to the tubular system has been described. It is also possible that the inward-going rectification is the intrinsic property of the plasma membrane. Inactivation of the K conductance has been noted as a fourth property of the active membrane of the excitable cell (Grundfest, 1960, 1961), as clearly demonstrated in the frog striated muscle and in the puffer fish neurons (Nakajima *et al.* 1962; Nakajima & Kusano, 1966; Nakajima, 1966). After complete inactivation of the delayed rectification, the steady state $I-V$ relation in frog skeletal muscle shows inward-going rectification in a certain range of the membrane potential (Nakajima *et al.* 1962; Adrian *et al.* 1970). Thus the inward-going rectification may well be a concomitant attribute of delayed potassium rectification. However, there is evidence which distinguishes the inward rectifying conductance from the outward rectifying conductance. In the frog striated muscle, internal K was exchanged with Rb and it was found that Rb can replace K for the delayed rectification, while the inward-going K rectification was eliminated in Rb-Ringer solution (Adrian, 1964; Adrian *et al.* 1970). In electro-plaque membrane as well, the inward rectifying conductances have been abolished by the replacement of K ions with Rb ions (Nakamura *et al.* 1965). In this tunicate the inward-going rectification of the embryonic membrane was also markedly suppressed in the Rb ASW.

All above mentioned points strongly suggest that the essentially same inward-going K rectification as initially found in frog skeletal muscle fibres actually originates in the embryonic membrane and may be an intrinsic property of the plasma membrane.

We thank Professor S. Hagiwara, Professor A. Grinnell, Dr Y. Kidokoro and Dr D. Eaton for their kind help in preparing the manuscript. We also thank Professor A. Takeuchi for useful comments on the manuscript. This work was supported by the grant from the Education Ministry of Japan.

REFERENCES

ADRIAN, R. H. (1964). The rubidium and potassium permeability of frog muscle membrane. *J. Physiol.* **175**, 134–159.

ADRIAN, R. H. (1969). Rectification in muscle membrane. *Prog. Biophys. molec. Biol.* **19**, 339–369.

ADRIAN, R. H., CHANDLER, W. K. & HODGKIN, A. L. (1970). Slow changes in potassium permeability in skeletal muscle. *J. Physiol.* **208**, 645–668.

ADRIAN, R. H. & FREYGANG, W. H. (1962*a*). The potassium and chloride conductance of frog muscle membrane. *J. Physiol.* **163**, 61–103.

ADRIAN, R. H. & FREYGANG, W. H. (1962*b*). Potassium conductance of frog muscle membrane under controlled voltage. *J. Physiol.* **163**, 104–114.

ASHMAN, R. F., KANNO, Y. & LOEWENSTEIN, W. R. (1964). The intercellular electrical coupling at a forming membrane junction in a dividing cell. *Science, N.Y.* **145**, 604–605.

BENNETT, M. V. L. & GRUNDFEST, H. (1966). Analysis of depolarizing and hyperpolarizing inactivation responses in gymnotid electroplaques. *J. gen. Physiol.* **50**, 141–169.

BENNETT, M. V. L. & TRINKAUS, J. P. (1970). Electrical coupling between embryonic cells by way of extracellular space and specialized junctions. *J. cell Biol.* **44**, 529–610.

CARMELIET, E. (1961). Chloride ions and the membrane potential of Purkinje fibres. *J. Physiol.* **156**, 375–388.

CONKLIN, E. G. (1905). The organization and cell-lineage of the ascidian egg. *J. Acad. nat. Sci. Philad.* **12**, 1–119.

DECK, K. A. & TRAUTWEIN, W. (1964). Ionic currents in cardiac excitation. *Pflügers Arch. ges. Physiol.* **280**, 63–80.

EISENBERG, R. S. & GAGE, P. W. (1969). Ionic conductances of the surface and transverse tubular membranes of frog sartorius fibers. *J. gen. Physiol.* **53**, 279–297.

GRUNDFEST, H. (1960). A four-factor ionic hypothesis of spike electrogenesis. *Biol. Bull. mar. biol. Lab. Woods Hole* **119**, 284.

GRUNDFEST, H. (1961). Ionic mechanisms in electrogenesis. *Ann. N.Y. Acad. Sci.* **94**, 405–457.

GRUNDFEST, H. (1966). Heterogeneity of excitable membrane: electrophysiological and pharmacological evidence and some consequences. *Ann. N.Y. Acad. Sci.* **131**, 901–949.

HALL, A. E., HUTTER, O. F. & NOBLE, D. (1963). Current–voltage relations of Purkinje fibres in sodium-deficient solutions. *J. Physiol.* **166**, 225–240.

HODGKIN, A. L. & HOROWICZ, P. (1959). The influence of potassium and chloride ions on the membrane potential of single muscle fibres. *J. Physiol* **148**, 127–160.

HUTTER, O. F. & NOBLE, D. (1960). Rectifying properties of cardiac muscle. *Nature, Lond.* **188**, 495.

ITO, S. & HORI, N. (1966). Electrical characteristics of Triturus egg during cleavage. *J. gen. Physiol.* **49**, 1019–1027.

ITO, S. & LOEWENSTEIN, W. R. (1969). Ionic communication between early embryonic cells. *Devl Biol.* **19**, 228–243.

KATZ, B. (1949). Les constantes éléctriques de la membrane du muscle. *Archs Sci. physiol.* **3**, 285–300.

LOEWENSTEIN, W. R. (1968). Communication through cell junctions. Implications in growth control and differentiation. *Devl Biol.* **2**, 151–183.

LOEWENSTEIN, W. R., NAKAS, M. & SOCOLAR, S. J. (1967). Junctional membrane uncoupling: permeability transformation at a cell membrane junction. *J. gen. Physiol.* **50**, 1865–1891.

MIYAZAKI, S., TAKAHASHI, K. & TSUDA, K. (1972). Calcium and sodium contributions to regenerative responses in the embryonic excitable cell membrane. *Science, N.Y.* **176**, 1441–1443.

MIYAZAKI, S., TAKAHASHI, K. & TSUDA, K. (1974). Electrical excitability in the egg cell membrane of the tunicate. *J. Physiol.* **238**, 37–54.

NAKAJIMA, S. (1966). Analysis of K inactivation and TEA action in the supramedullary cells of puffer. *J. gen. Physiol.* **49**, 629–640.

NAKAJIMA, S., IWASAKI, S. & OBATA, K. (1962). Delayed rectification and anomalous rectification in frog skeletal muscle membrane. *J. gen. Physiol.* **46**, 97–115.

NAKAJIMA, S. & KUSANO, K. (1966). Behavior of delayed current under voltage clamp in the supramedullary neurons of puffer. *J. gen. Physiol.* **47**, 613–628.

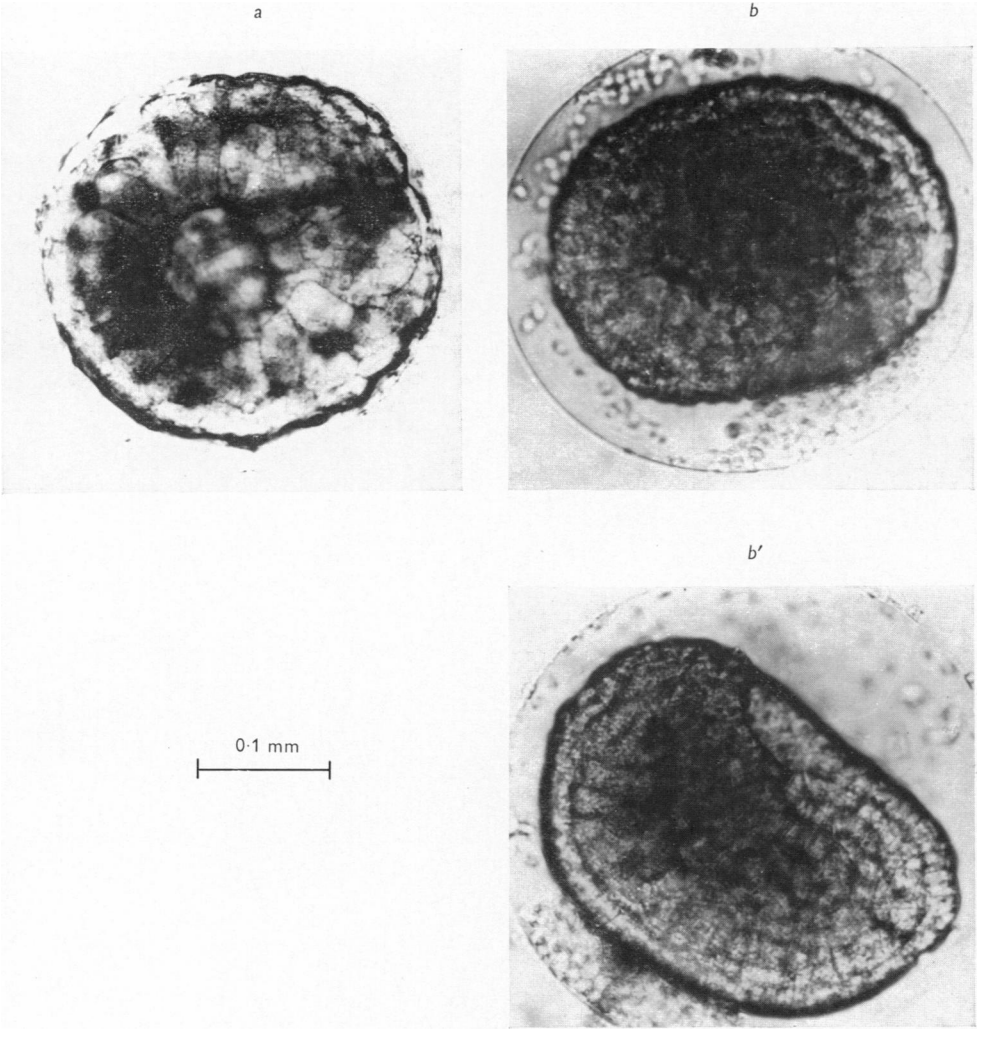
a
b
b'
0·1 mm

NAKAMURA, Y., NAKAJIMA, S. & GRUNDFEST, H. (1965). Analysis of spike electrogenesis and depolarizing K inactivation in electroplaques of electrophorus electricus, L. *J. gen. Physiol.* **49**, 321–349.

NOBLE, D. (1965). Electrical properties of cardiac muscle attributable to inward going (Anomalous) rectification. *J. cell. comp. Physiol.* **66**, 127–136.

NOBLE, D. & TSIEN, R. W. (1968). The kinetics and rectifier properties of the slow potassium current in cardiac Purkinje fibres. *J. Physiol.* **195**, 185–214.

PALMER, J. F. & SLACK, C. (1970). Some bio-electric parameters of early Xenopus embryos. *J. Embryol. exp. Morph.* **24**, 535–558.

POTTER, D. D., FURSHPAN, E. J. & LENNOX, E. S. (1966). Connections between cells of the developing squid as revealed by electrophysiological methods. *Proc. natn. Acad. Sci. U.S.A.* **55**, 328–336.

ROSE, B. & LOEWENSTEIN, W. R. (1971). Junctional membrane permeability: Depression by substitution of Li for extracellular Na and by long term lack of Ca and Mg; Restoration by cell repolarization. *J. membrane Biol.* **5**, 20–50.

SHERIDAN, J. D. (1966). Electrophysiological study of special connections between cells in the early embryo. *J. cell Biol.* **31**, C1–C5.

SHERIDAN, J. D. (1968). Electrophysiological evidence for low-resistance intercellular junctions in the early chick embryo. *J. cell Biol.* **31**, 650–659.

SHERIDAN, J. D. (1971). Dye movement and low-resistance junctions between reaggregated embryonic cells. *Devl Biol.* **26**, 627–636.

SLACK, C. & PALMER, J. P. (1969). The permeability of intercellular junctions in the early embryo of *Xenopus laevis*, studied with a fluorescent tracer. *Expl Cell Res.* **55**, 416–419.

TAKAHASHI, K., MIYAZAKI, S. & KIDOKORO, Y. (1971). Development of excitability in embryonic muscle cell membranes in certain tunicates. *Science, N.Y.* **171**, 415–418.

TRAUTWEIN, W. & KASSEBAUM, D. G. (1961). On the mechanism of spontaneous impulse generation in the pacemaker of the heart. *J. gen. Physiol.* **45**, 317–330.

TUPPER, J., SAUNDERS, J. W., Jr. & EDWARDS, C. (1970). The onset of electrical coupling between cells in the developing starfish embryo. *J. cell Biol.* **46**, 187–190.

WARNER, A. E. (1970). Electrical connexions between cells at neural stage of the axolotl. *J. Physiol.* **210**, 150–151*P*.

WEIDMANN, S. (1955). Rectifier properties of Purkinje fibers. *Am. J. Physiol.* **183**, 671.

WEIDMANN, S. (1956). *Electrophysiologie der Herzmuskelfaser*. Bern: Huber.

EXPLANATION OF PLATE

Photographs of embryos at the stage of gastrula. Photographs *a*, *b*, *b′* illustrate an early gastrula with a widely opened blastopore and dorsal and side views of a middle stage gastrula with a slightly opened blastopore respectively.